A Perturbative Solution to Plane Wave Scattering From a Rough Dielectric Cylinder

Rahul Trivedi and Uday K. Khankhoje

***Abstract*—We present an analytical, second-order perturbative solution to the problem of electromagnetic plane-wave scattering from a dielectric cylinder with a randomly rough surface. In contrast to previous integral equation-based approaches, we perturb the electromagnetic boundary conditions at the cylinder interface. Doing so affords us tractable expressions for the fields internal and external to the cylinder. We validate our results by comparing them with rigorous, but computationally intensive solutions obtained from the method of moments, and numerically estimate a region of validity for our results. We report this region as $h_0 < \lambda/20$ and $l > 4\,h_0$, where h_0 and l are the root-mean-square surface roughness and surface correlation length, respectively, for scattering at a wavelength λ.**

***Index Terms*—Electromagnetic scattering by rough surfaces, integral equations, perturbation methods.**

I. Introduction

VEGETATION is an important contributor to radar scattering. This scattering comprises contributions from leaves, branches, and tree trunks. In the case of branches and trunks, it is common to model them as conducting or dielectric cylinders that have either rough or smooth surfaces. The choice of model depends upon the radar wavelength, the relative size of the trunk, and the statistical properties (mean roughness, etc.) of the trunk's surface.

At low microwave frequencies, tree trunks are modeled as smooth, dielectric cylinders of finite length [1], [2]. At higher frequencies, when the surface roughness becomes comparable to the wavelength, it is important to model the roughness of the cylinder surface. Some studies have modeled the roughness as a periodic corrugation in a dielectric layer [3], [4]. This assumption is harder to justify at the higher frequencies encountered in millimeter wave scattering, and models for the scattered fields have been developed using geometric-optics approximations [5].

The small perturbation method (SPM) was originally developed in the context of modeling scattering by slightly rough surfaces [6]–[8]. The SPM as applied to rough surfaces falls in the general category of *geometrical properties perturbation* [9], [10] wherein the material properties of the perturbed scatterer are the same as that of the unperturbed scatterer, with the perturbation appearing only in the boundaries of the scatterer. This is in contrast to the problems involving *dielectric properties perturbation* [11], wherein the dielectric properties of the scatterer are treated perturbatively. The SPM has also been applied to model rough perfect electrically conducting (PEC) cylinders; to first-order by Cabayan and Murphy [12], and to second-order by Eftimiu [13] and [14] and to cylinders with an impedance boundary condition by Tong [15]. The SPM method breaks down as the surface roughness increases, and in such cases, a full-wave solution is desirable [16].

In this paper, we develop a second-order SPM scheme for calculating the fields scattered from a randomly rough dielectric cylinder of infinite height. While several authors have used the SPM to first- and second-order for the analysis of azimuthally rough cylinders modeled as PEC cylinders or as impedance surfaces, there has been no previous report of an SPM analysis of a rough *dielectric* cylinder with azimuthal and z-dependent roughness. Moreover, the existing SPM for rough PEC cylinders is based on the integral equation formulation of the scattering problem, whereas our approach is to perturb the boundary conditions at the cylinder surface which, in general, yield more tractable solutions in the case of a dielectric cylinder with azimuthal and z-dependent roughness as compared to the integral equation method. We note that in the reduced case of a PEC cylinder, our method simplifies to the previously reported results [12]–[14]. Additionally, since our method yields not only the scattered fields but also the fields inside the rough dielectric cylinder, it can easily be extended to finite rough cylinders by using an approach similar to that used by Hulst and Van De Hulst [17] and Seker and Schneider [18] in their treatment of finite smooth cylinders.

Section II presents the formulation of the scattering problem as a boundary value problem. The boundary conditions at the interface of the dielectric and vacuum are perturbed to obtain zeroth-, first-, and second-order boundary conditions which, in turn, are used to evaluate the scattered electromagnetic fields up till the second-order. In Section III, we numerically validate the perturbative solution by comparing it with an accurate integral equation (or method of moments—MoM) method for the special cases of small azimuthal or axial roughness. A region of validity for the second-order perturbative solution is also numerically estimated in Section IV by comparing it with the integral equation method. Finally, we conclude this paper with general observations regarding the computational efficiency and applicability of our SPM analysis as compared to existing exact numerical methods.

Manuscript received January 06, 2015; revised May 15, 2015; accepted June 24, 2015. Date of publication July 06, 2015; date of current version September 01, 2015. The work of U. K. Khankhoje was supported from INSPIRE Faculty Award (IFA-13 ENG-60) by the Department of Science and Technology, Government of India.

The authors are with the Department of Electrical Engineering, Indian Institute of Technology Delhi, New Delhi 110016, India (e-mail: ee1120469@ee.iitd.ac.in; uday@alumni.caltech.edu).

Digital Object Identifier 10.1109/TAP.2015.2452968

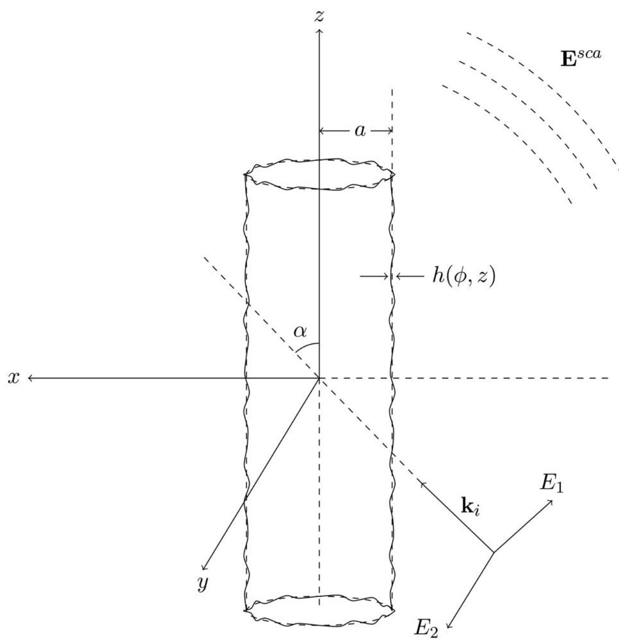

Fig. 1. Schematic of the rough cylindrical scatterer with a stochastic roughness $h(\phi, z)$ and illuminated by a plane wave propagating with wavevector $\mathbf{k}_i$ in the xz-plane at an angle of α with the x-axis. E_1 is the component of the electric field in the xz-plane, while E_2 is the component along the y-axis.

II. PERTURBATIVE METHOD

The scatterer of interest is an infinitely long rough cylinder with mean radius a. The roughness is described by a zero mean stochastic process, $h(\phi, z)$. As shown in Fig. 1, $a + h(\phi, z)$ is the radial distance of a point on the rough cylinder surface. Throughout this paper, r, ϕ, and z denote the radial, azimuthal, and height coordinates, respectively. An instance of the stochastic process $h(\phi, z)$ can be expressed as

$$h(\phi, z) = \sum_{n=-\infty}^{\infty} \int_{-\infty}^{\infty} \tilde{h}_n(k) \exp(j(kz + n\phi))dk \tag{1a}$$

$$\tilde{h}_n(k) = \frac{1}{4\pi^2} \int_{z=-\infty}^{\infty} \int_{\phi=0}^{2\pi} h(\phi, z) \exp(-j(n\phi + kz))\, d\phi\, dz. \tag{1b}$$

Additionally, note that since $h(\phi, z)$ is real $\forall \phi \in (0, 2\pi]$, $z \in \mathbb{R}$

$$\tilde{h}_{-n}(k) = \tilde{h}_n^*(k) \text{ and } \tilde{h}_n(-k) = \tilde{h}_n^*(k). \tag{2}$$

The permittivity and permeability of the cylinder are assumed to be uniform, and given by ϵ_d and μ_d and it is assumed that the cylinder is placed in vacuum. $k_0 = \sqrt{\epsilon_0 \mu_0 \omega^2}$ and $\eta_0 = \sqrt{\mu_0/\epsilon_0}$ denote the wave number and wave impedance in vacuum, and $k_d = \sqrt{\epsilon_d \mu_d \omega^2}$ and $\eta_d = \sqrt{\mu_d/\epsilon_d}$ denote the same in the dielectric.

In the analysis that follows, we determine the scattered electric and magnetic fields to the second-order in $h(\phi, z)$ for an arbitrary but deterministic roughness function. Once the response of the cylinder is known in terms of $h(\phi, z)$, the statistical averages of the scattered fields and derived quantities (such as the scattering cross section) can be expressed in terms of the statistical averages of the stochastic process $h(\phi, z)$.

A. Formulation of Boundary Conditions on a Perturbed Surface

In this section, we present a modified set of boundary conditions that can be used to perturbatively evaluate the scattered fields for a given incident field. Let the fields outside and inside the cylinder be denoted by $\mathbf{E}_I$, $\mathbf{H}_I$ and $\mathbf{E}_{II}$, $\mathbf{H}_{II}$, respectively. A sufficient set of boundary conditions to solve the scattering problem evaluated at the cylinder surface, $r = a + h(\phi, z)$, is

$$\Delta\mathbf{E} \times \mathbf{n}|_{r=a+h} = 0 \tag{3a}$$

$$\Delta\mathbf{H} \times \mathbf{n}|_{r=a+h} = 0 \tag{3b}$$

where $\Delta\mathbf{E} = \mathbf{E}_I - \mathbf{E}_{II}$ and $\Delta\mathbf{H} = \mathbf{H}_I - \mathbf{H}_{II}$ and $\mathbf{n}$ is the outward normal to the cylinder surface at the point $(a + h(\phi, z), \phi, z)$

$$\mathbf{n} = \hat{r} - \left(\frac{1}{a+h}\right)\frac{\partial h}{\partial \phi}\hat{\phi} - \frac{\partial h}{\partial z}\hat{z}. \tag{4}$$

Equation (3a) can be rewritten in terms of the components of $\mathbf{E}$ and $\mathbf{H}$ as follows:

$$\Delta E_z \Big|_{r=a+h} = -\frac{\partial h}{\partial z}\Delta E_r\Big|_{r=a+h} \tag{5a}$$

$$(a+h)\Delta E_\phi \Big|_{r=a+h} = -\frac{\partial h}{\partial \phi}\Delta E_r\Big|_{r=a+h} \tag{5b}$$

$$\Delta H_z\Big|_{r=a+h} = -\frac{\partial h}{\partial z}\Delta H_r\Big|_{r=a+h} \tag{5c}$$

$$(a+h)\Delta H_\phi\Big|_{r=a+h} = -\frac{\partial h}{\partial \phi}\Delta H_r\Big|_{r=a+h}. \tag{5d}$$

For $h \ll a$, the Taylor series expansion along with (5a) yields

$$\Delta E_z\Big|_{r=a} + h\frac{\partial \Delta E_z}{\partial r}\Big|_{r=a} + \frac{h^2}{2}\frac{\partial^2 \Delta E_z}{\partial r^2}\Big|_{r=a} = -\frac{\partial h}{\partial z}\Delta E_r\Big|_{r=a} - h\frac{\partial h}{\partial z}\frac{\partial \Delta E_r}{\partial r}\Big|_{r=a} \tag{6a}$$

$$\Delta E_\phi\Big|_{r=a} + \frac{h}{a}\Delta E_\phi\Big|_{r=a} + h\frac{\partial \Delta E_\phi}{\partial r}\Big|_{r=a} + \frac{h^2}{2}\frac{\partial^2 \Delta E_\phi}{\partial r^2}\Big|_{r=a} + \frac{h^2}{a}\frac{\partial \Delta E_\phi}{\partial r}\Big|_{r=a} = -\frac{1}{a}\frac{\partial h}{\partial \phi}\Delta E_r\Big|_{r=a} - \frac{h}{a}\frac{\partial h}{\partial \phi}\frac{\partial \Delta E_r}{\partial r}\Big|_{r=a} \tag{6b}$$

$$\Delta H_z\Big|_{r=a} + h\frac{\partial \Delta H_z}{\partial r}\Big|_{r=a} + \frac{h^2}{2}\frac{\partial^2 \Delta H_z}{\partial r^2}\Big|_{r=a} = -\frac{\partial h}{\partial z}\Delta H_r\Big|_{r=a} - h\frac{\partial h}{\partial z}\frac{\partial \Delta H_r}{\partial r}\Big|_{r=a} \tag{6c}$$

$$\Delta H_\phi\Big|_{r=a} + \frac{h}{a}\Delta H_\phi\Big|_{r=a} + h\frac{\partial \Delta H_\phi}{\partial r}\Big|_{r=a} + \frac{h^2}{2}\frac{\partial^2 \Delta H_\phi}{\partial r^2}\Big|_{r=a} + \frac{h^2}{a}\frac{\partial \Delta H_\phi}{\partial r}\Big|_{r=a} = -\frac{1}{a}\frac{\partial h}{\partial \phi}\Delta H_r\Big|_{r=a} - \frac{h}{a}\frac{\partial h}{\partial \phi}\frac{\partial \Delta H_r}{\partial r}\Big|_{r=a}. \tag{6d}$$

The functions $\Delta\mathbf{E}$ and $\Delta\mathbf{H}$ can be expanded as a perturbation series as follows:

$$\Delta\mathbf{E} = \Delta\mathbf{E}^{(0)} + \Delta\mathbf{E}^{(1)} + \cdots \tag{7a}$$

$$\Delta\mathbf{H} = \Delta\mathbf{H}^{(0)} + \Delta\mathbf{H}^{(1)} + \cdots \tag{7b}$$

where $\Delta\mathbf{E}^{(m)}$ or $\Delta\mathbf{H}^{(m)}$ is of the order of h^m. Using (6a) along with (7a), the boundary conditions may be formulated in terms of the perturbations in $\Delta\mathbf{E}$ and $\Delta\mathbf{H}$.

1) Zeroth-Order Boundary Conditions:

$$\Delta E_z^{(0)}\Big|_{r=a} = 0 = \Delta E_\phi^{(0)}\Big|_{r=a} \tag{8a}$$

$$\Delta H_z^{(0)}\Big|_{r=a} = 0 = \Delta H_\phi^{(0)}\Big|_{r=a}. \tag{8b}$$

2) First-Order Boundary Conditions:

$$\Delta E_z^{(1)}\Big|_{r=a} = -h\frac{\partial \Delta E_z^{(0)}}{\partial r}\Big|_{r=a} - \frac{\partial h}{\partial z}\Delta E_r^{(0)}\Big|_{r=a} \tag{9a}$$

$$\Delta E_\phi^{(1)}\Big|_{r=a} = -h\frac{\partial \Delta E_\phi^{(0)}}{\partial r}\Big|_{r=a} - \frac{1}{a}\frac{\partial h}{\partial \phi}\Delta E_r^{(0)}\Big|_{r=a} \tag{9b}$$

$$\Delta H_z^{(1)}\Big|_{r=a} = -h\frac{\partial \Delta H_z^{(0)}}{\partial r}\Big|_{r=a} - \frac{\partial h}{\partial z}\Delta H_r^{(0)}\Big|_{r=a} \tag{9c}$$

$$\Delta H_\phi^{(1)}\Big|_{r=a} = -h\frac{\partial \Delta H_\phi^{(0)}}{\partial r}\Big|_{r=a} - \frac{1}{a}\frac{\partial h}{\partial \phi}\Delta H_r^{(0)}\Big|_{r=a}. \tag{9d}$$

3) Second-Order Boundary Conditions:

$$\Delta E_z^{(2)}\Big|_{r=a} = -h\frac{\partial \Delta E_z^{(1)}}{\partial r}\Big|_{r=a} - \frac{h^2}{2}\frac{\partial^2 \Delta E_z^{(0)}}{\partial r^2}\Big|_{r=a} - \frac{\partial h}{\partial z}\Delta E_r^{(1)}\Big|_{r=a} - h\frac{\partial h}{\partial z}\frac{\partial \Delta E_r^{(0)}}{\partial r}\Big|_{r=a} \tag{10a}$$

$$\Delta E_\phi^{(2)}\Big|_{r=a} = -h\frac{\partial \Delta E_\phi^{(1)}}{\partial r}\Big|_{r=a} - \frac{h^2}{2}\frac{\partial^2 \Delta E_\phi^{(0)}}{\partial r^2}\Big|_{r=a} - \frac{1}{a}\frac{\partial h}{\partial \phi}\Delta E_r^{(1)}\Big|_{r=a} + \frac{h}{a^2}\frac{\partial h}{\partial \phi}\Delta E_r^{(0)}\Big|_{r=a} - \frac{h}{a}\frac{\partial h}{\partial \phi}\frac{\partial \Delta E_r^{(0)}}{\partial r}\Big|_{r=a} \tag{10b}$$

$$\Delta H_z^{(2)}\Big|_{r=a} = -h\frac{\partial \Delta H_z^{(1)}}{\partial r}\Big|_{r=a} - \frac{h^2}{2}\frac{\partial^2 \Delta H_z^{(0)}}{\partial r^2}\Big|_{r=a} - \frac{\partial h}{\partial z}\Delta H_r^{(1)}\Big|_{r=a} - h\frac{\partial h}{\partial z}\frac{\partial \Delta H_r^{(0)}}{\partial r}\Big|_{r=a} \tag{10c}$$

$$\Delta H_\phi^{(2)}\Big|_{r=a} = -h\frac{\partial \Delta H_\phi^{(1)}}{\partial r}\Big|_{r=a} - \frac{h^2}{2}\frac{\partial^2 \Delta H_\phi^{(0)}}{\partial r^2}\Big|_{r=a} - \frac{1}{a}\frac{\partial h}{\partial \phi}\Delta H_r^{(1)}\Big|_{r=a} + \frac{h}{a^2}\frac{\partial h}{\partial \phi}\Delta H_r^{(0)}\Big|_{r=a} - \frac{h}{a}\frac{\partial h}{\partial \phi}\frac{\partial \Delta H_r^{(0)}}{\partial r}\Big|_{r=a}. \tag{10d}$$

Equations (8)–(10) are the sets of boundary conditions that will be used in solving the scattering problem. Also note that these conditions are valid irrespective of the dielectric properties of the cylinder. For instance, the case of a PEC cylinder is handled by using these boundary conditions with the internal fields set to zero; we use this property in Section III-B. Higher order perturbed boundary conditions can be similarly derived if desired, but we restrict our analysis to up till second-order in $h(\phi, z)$.

B. Scattering of a Plane Wave by the Rough Cylinder

Consider an electromagnetic plane wave incident at an angle α with the z-axis, and the incident wavevector $\mathbf{k}_i$, being in the xz-plane, as shown in Fig. 1. The incident fields $\mathbf{E}^{inc}$ and $\mathbf{H}^{inc}$ may be expressed as

$$\mathbf{E}^{inc} = (E_1(\hat{z}\sin\alpha - \hat{x}\cos\alpha) + E_2\hat{y})\exp(j\mathbf{k}_i\cdot\mathbf{r}) \tag{11a}$$

$$\mathbf{H}^{inc} = \frac{(-E_1\hat{y} + E_2(-\hat{x}\cos\alpha + \hat{z}\sin\alpha))}{\eta_0}\exp(j\mathbf{k}_i\cdot\mathbf{r}) \tag{11b}$$

where E_1 and E_2 are as per Fig. 1. A time dependance of $\exp(-j\omega t)$ is assumed in all the fields and suppressed throughout the paper.

It is known that in homogenous dielectric media, the z components of the electric and magnetic fields satisfy the scalar Helmholtz equation ($k_m = \sqrt{\mu_m \epsilon_m \omega^2}$ is the wave number of the medium)

$$\nabla^2 v + k_m^2 v = 0 \quad \text{for } v \equiv E_z \text{ or } H_z. \tag{11}$$

The eigen solutions of (12) in the cylindrical coordinates are given by

$$v_z = Z_n(\beta_m r)\exp(jn\phi)\exp(jkz) \tag{12}$$

where $\beta_m = \sqrt{k_m^2 - k^2}\,\forall\ k \in \mathbb{R}$ and $n \in \mathbb{Z}$ and $Z_n(x)$ are solutions of the Bessel differential equations of order n. A general solution of (12) can therefore be expressed as a linear combination of the eigen-solutions given by (13)

$$v_z = \sum_{n=-\infty}^{\infty}\int_{-\infty}^{\infty}\Big[a_n(k)H_n^{(1)}(\beta_m r) + b_n(k)J_n(\beta_m r)\Big] \exp(jkz)\exp(jn\phi)\,dk \tag{13}$$

where $H_n^{(1)}$ and J_n are the nth order Hankel function (of the first kind) and the Bessel function, respectively. A complete representation of the general solution, as shown in (14), would require an integration over eigen-solutions with a z dependance of the form $\exp(jkz)$ (since k is a continuous index) in addition to the summation over the eigen-solution with a ϕ dependance of the form $\exp(jn\phi)$. $a_n(k)$ and $b_n(k)$ are the *weights* of the corresponding eigen-solution in the net field. In general, we will have four unknown weight functions [$a_n(k)$ and $b_n(k)$ for $v \equiv E_z$ and H_z] in a complete representation of the fields corresponding to the four independent solutions of Maxwell's equations [19]; these will be evaluated by applying the boundary conditions at the medium interfaces and the radiation condition at infinity. Moreover, once E_z and H_z are known, the other components of E and H, namely E_r, E_ϕ, H_r, and H_ϕ can be readily determined in terms of E_z and H_z (refer to Appendix A for the actual expressions) and therefore, it is sufficient to formulate and solve the scattering problem in terms of E_z and H_z alone and use them to evaluate all the other components.

The z components of the incident fields from (11), E_z^{inc} and H_z^{inc}, can be expressed as a linear combination of the form in (14) using the Jacobi–Anger expansion

$$E_z^{inc} = E_1 \sin\alpha \sum_{n=-\infty}^{\infty} j^n J_n(k_0 r \sin\alpha) \exp(jn\phi) \exp(jk_0 z \cos\alpha) \tag{15a}$$

$$H_z^{inc} = \frac{E_2}{\eta_0} \sin\alpha \sum_{n=-\infty}^{\infty} j^n J_n(k_0 r \sin\alpha) \exp(jn\phi) \exp(jk_0 z \cos\alpha). \tag{15b}$$

The fields in the medium surrounding the cylinder can be expressed as a superposition of the known incident field described above and an unknown scattered field. The scattered fields E_z^{sca} and H_z^{sca} can be expressed as

$$E_z^{sca} = \sum_{n=-\infty}^{\infty} \int_{-\infty}^{\infty} s_n(k) H_n^{(1)}(\beta_0 r) \exp(j(kz + n\phi))\, dk \tag{16a}$$

$$H_z^{sca} = \sum_{n=-\infty}^{\infty} \int_{-\infty}^{\infty} g_n(k) H_n^{(1)}(\beta_0 r) \exp(j(kz + n\phi))\, dk \tag{16b}$$

where $\beta_0 = \sqrt{k_0^2 - k^2}$ and $g_n(k)$ and $s_n(k)$ are the (unknown) weights of the corresponding eigen-solution in the scattered field.

The fields in the interior of the cylinder E_z^{cyl} and H_z^{cyl} can be expressed as

$$E_z^{cyl} = \sum_{n=-\infty}^{\infty} \int_{-\infty}^{\infty} a_n(k) J_n(\beta_d r) \exp(j(kz + n\phi))\, dk \tag{17a}$$

$$H_z^{cyl} = \sum_{n=-\infty}^{\infty} \int_{-\infty}^{\infty} b_n(k) J_n(\beta_d r) \exp(j(kz + n\phi))\, dk \tag{17b}$$

where $\beta_d = \sqrt{k_d^2 - k^2}$ and $b_n(k)$ and $a_n(k)$ are the weights of the corresponding eigen-solution in the interior field.

To evaluate $s_n(k)$, $g_n(k)$, $a_n(k)$, and $b_n(k)$, we will make use of the perturbed boundary conditions given by (8)–(10). Consequently, it is necessary to expand these coefficients into a perturbation series

$$f_n(k) = \sum_{m=0}^{\infty} f_n^{(m)}(k) \quad \forall n \in \mathbb{Z}, k \in \mathbb{R} \text{ and } f \in \{s, g, a, b\} \tag{17}$$

where, by assumption, $f_n^{(m)}(k) \sim O(h^m)$. We emphasize that the coefficient of *each* eigenfunction in the field expansion is expressed as a perturbation series. $f_n^{(0)}(k)$ can be evaluated via the application of (8) and then can be used to evaluate $\Delta\mathbf{E}^{(0)}$ and $\Delta\mathbf{H}^{(0)}$. These, in turn, can be used together with (9) to evaluate $f_n^{(1)}(k)$ and by extension $\Delta\mathbf{E}^{(1)}$ and $\Delta\mathbf{H}^{(1)}$. Subsequently, $f_n^{(2)}(k)$ can be obtained by the application of (10).

In the following sections, we present results for the zeroth-, first-, and second-order field coefficients, as given by $f_n^{(m)}$. Interested readers may refer to Appendix A for further details and derivations. To keep the equations that follow compact, we define a matrix $\mathbf{\Theta}_n(k)$

$$\mathbf{\Theta}_n(k) = [\mathbf{\Lambda}_{1,n}(k)\, \mathbf{\Lambda}_{2,n}(k)]^{-1} \tag{18}$$

where

$$\mathbf{\Lambda}_{1,n}(k) = \begin{bmatrix} H_n^{(1)}(\beta_0 a) & 0 \\ 0 & H_n^{(1)}(\beta_0 a) \\ \frac{-nk}{\beta_0^2 a} H_n^{(1)}(\beta_0 a) & \frac{-j\eta_0 k_0}{\beta_0} H_n^{(1)'}(\beta_0 a) \\ \frac{jk_0}{\beta_0 \eta_0} H_n^{(1)'}(\beta_0 a) & \frac{-nk}{\beta_0^2 a} H_n^{(1)}(\beta_0 a) \end{bmatrix} \tag{20a}$$

$$\mathbf{\Lambda}_{2,n}(k) = \begin{bmatrix} -J_n(\beta_d a) & 0 \\ 0 & -J_n(\beta_d a) \\ \frac{nk}{\beta_d^2 a} J_n(\beta_d a) & \frac{j\eta_d k_d}{\beta_d} J_n'(\beta_d a) \\ \frac{-jk_d}{\beta_d \eta_d} J_n'(\beta_d a) & \frac{nk}{\beta_d^2 a} J_n(\beta_d a) \end{bmatrix}. \tag{20b}$$

1) Zeroth-Order Field Coefficients: The boundary conditions given by (8) result in the following familiar result of specular scattering from a smooth cylinder [20]

$$f_n^{(0)}(k) = \sum_{i=1}^{2} F_{i,n}^{(0)}\, E_i\, \delta(k - k_0 \cos\alpha) \quad \text{for } f \in \{s, g, a, b\},\ F \in \{S, G, A, B\} \tag{21}$$

where

$$\begin{bmatrix} S_{1,n}^{(0)} \\ G_{1,n}^{(0)} \\ A_{1,n}^{(0)} \\ B_{1,n}^{(0)} \end{bmatrix} = \mathbf{\Theta}_n(k_0 \cos\alpha) \begin{bmatrix} -j^n J_n(k_0 a \sin\alpha) \sin\alpha \\ 0 \\ \frac{j^n n}{k_0 a} J_n(k_0 a \sin\alpha) \cot\alpha \\ \frac{-j^{n+1}}{\eta_0} J_n'(k_0 a \sin\alpha) \end{bmatrix} \tag{22}$$

$$\begin{bmatrix} S_{2,n}^{(0)} \\ G_{2,n}^{(0)} \\ A_{2,n}^{(0)} \\ B_{2,n}^{(0)} \end{bmatrix} = \mathbf{\Theta}_n(k_0\cos\alpha) \begin{bmatrix} 0 \\ \frac{-j^n}{\eta_0} J_n(k_0 a\sin\alpha)\sin\alpha \\ j^{n+1}J_n'(k_0 a\sin\alpha) \\ \frac{nj^n\cot\alpha}{\eta_0 k_0 a} J_n(k_0 a\sin\alpha) \end{bmatrix}. \quad (23)$$

2) First-Order Field Coefficients: Similarly, (9) can be used to formulate equations in the first-order perturbations in the coefficients. Let $Q_{i,n,X}^{(0)}(r)$ be defined by

$$\Delta X_q^{(0)}(r) = \sum_{n=-\infty}^{\infty}\sum_{i=1}^{2} E_i Q_{i,n,X}^{(0)}(r)\exp(j(n\phi + k_0 z\cos\alpha))$$
$$\text{for } X \in \{E,H\}, q \in \{r,\phi,z\}, Q \in \{R,\Phi,Z\}. \quad (24)$$

The first-order perturbation coefficients can be expressed as

$$f_n^{(1)}(k) = \sum_{m=-\infty}^{\infty}\sum_{i=1}^{2} F_{i,n,m}^{(1)}(k) E_i \tilde{h}_m(k - k_0\cos\alpha)$$
$$\text{for } f \in \{s,g,a,b\}, F \in \{S,G,A,B\} \quad (25)$$

where $F_{i,n,m}^{(1)}(k)$ satisfy (for $i = 1, 2$)

$$\begin{bmatrix} S_{i,n,m}^{(1)}(k) \\ G_{i,n,m}^{(1)}(k) \\ A_{i,n,m}^{(1)}(k) \\ B_{i,n,m}^{(1)}(k) \end{bmatrix} = \mathbf{\Theta}_n(k)[\mathbf{R}_{i,n,m}^{(1)}(k) + \mathbf{T}_{i,n,m}^{(1)}(k)] \quad (26)$$

with

$$\mathbf{R}_{i,n,m}^{(1)}(k) = \begin{bmatrix} -j(k - k_0\cos\alpha) R_{i,n-m,E}^{(0)}(a) \\ -j(k - k_0\cos\alpha) R_{i,n-m,H}^{(0)}(a) \\ -\frac{jm}{a} R_{i,n-m,E}^{(0)}(a) \\ -\frac{jm}{a} R_{i,n-m,H}^{(0)}(a) \end{bmatrix} \quad (27a)$$

$$\mathbf{T}_{i,n,m}^{(1)}(k) = \begin{bmatrix} -Z_{i,n-m,E}^{(0)'}(a) \\ -Z_{i,n-m,H}^{(0)'}(a) \\ -\Phi_{i,n-m,E}^{(0)'}(a) \\ -\Phi_{i,n-m,H}^{(0)'}(a) \end{bmatrix}. \quad (27b)$$

3) Second-Order Field Coefficients: For second-order coefficients, we impose (10a). Clearly, the functions $\Delta\mathbf{E}^{(1)}$ and $\Delta\mathbf{H}^{(1)}$ are of the form

$$\Delta X_q^{(1)}(r) = \sum_{n=-\infty}^{\infty}\sum_{m=-\infty}^{\infty}\sum_{i=1}^{2}\int_{-\infty}^{\infty} E_i Q_{i,n,m,X}^{(1)}(r,k)$$
$$\tilde{h}_m(k - k_0\cos\alpha)\exp(j(n\phi + kz))\,dk$$
$$\text{for } X \in \{E,H\}, q \in \{r,\phi,z\}, Q \in \{R,\Phi,Z\}. \quad (28)$$

The second-order perturbation coefficients can be expressed as

$$f_n^{(2)}(k) = \sum_{m=-\infty}^{\infty}\sum_{p=-\infty}^{\infty}\sum_{i=1}^{2}\int_{-\infty}^{\infty} F_{i,n,m,p}^{(2)}(k,k')E_i$$
$$\tilde{h}_m(k' - k_0\cos\alpha)\tilde{h}_p(k - k')\,dk'$$
$$\text{for } f \in \{s,g,a,b\}, F \in \{S,G,A,B\} \quad (29)$$

where

$$\begin{bmatrix} S_{i,n,m,p}^{(2)}(k,k') \\ G_{i,n,m,p}^{(2)}(k,k') \\ A_{i,n,m,p}^{(2)}(k,k') \\ B_{i,n,m,p}^{(2)}(k,k') \end{bmatrix} = \mathbf{\Theta}_n(k)\Big[\mathbf{R}_{i,n,m,p}^{(2)}(k,k') + \mathbf{T}_{i,n,m,p}^{(2)}(k,k')\Big] \quad (30)$$

with

$$\mathbf{R}_{i,n,m,p}^{(2)}(k,k') = \begin{bmatrix} j(k'-k)(R_{i,n-p,m,E}^{(1)}(a,k') + R_{i,n-p-m,E}^{(0)'}(a)) \\ j(k'-k)(R_{i,n-p,m,E}^{(1)}(a,k') + R_{i,n-p-m,E}^{(0)'}(a)) \\ \frac{jp}{a^2}(R_{i,n-p-m,E}^{(0)}(a) - aR_{i,n-p-m,E}^{(0)'}(a) - aR_{i,n-p,m,E}^{(1)}(a)) \\ \frac{jp}{a^2}(R_{i,n-p-m,H}^{(0)}(a) - aR_{i,n-p-m,H}^{(0)'}(a) - aR_{i,n-p,m,H}^{(1)}(a)) \end{bmatrix} \quad (31a)$$

$$\mathbf{T}_{i,n,m,p}^{(2)}(k,k') = \begin{bmatrix} -Z_{i,n-p,m,E}^{(1)'}(a,k') - \frac{Z_{i,n-p-m,E}^{(0)''}(a)}{2} \\ -Z_{i,n-p,m,E}^{(1)'}(a,k') - \frac{Z_{i,n-p-m,E}^{(0)''}(a)}{2} \\ -\Phi_{i,n-p,m,E}^{(1)'}(a,k') - \frac{1}{2}\Phi_{i,n-m-p,E}^{(0)''}(a) \\ -\Phi_{i,n-p,m,H}^{(1)'}(a,k') - \frac{1}{2}\Phi_{i,n-m-p,H}^{(0)''}(a) \end{bmatrix} \quad (31b)$$

III. Validation

To validate the perturbative solution derived in the previous section and to establish criteria for its validity, we compare it with a rigorous MoM solution of the same problem [21]. For simplicity, we separately treat the cases where the cylinder has only an azimuthal roughness (i.e., h is independent of z) or an axial roughness (i.e., h is independent of ϕ).

A. Cylinder With Azimuthal Roughness

Consider a special case where the cylinder is only azimuthally rough

$$\tilde{h}_n(k) = h_n\delta(k) \quad \forall n \in \mathbb{Z}. \quad (32)$$

Additionally, assume that the incident field propagates in the x-direction with the electric field being polarized along the z-axis ($\alpha = \pi/2$, $E_2 = 0$). It can immediately be seen that in this particular case, the scattered fields are independent of z and $H_z^{sca} = H_z^{cyl} = 0$, i.e.,

$$f_n(k) = \begin{cases} F_n \delta(k) & \text{for } f \in \{s, a\}, F \in \{S, A\} \\ 0 & \text{for } f \in \{g, b\}. \end{cases} \tag{33}$$

Using (16a), the scattered field E_z^{sca} can be expressed as

$$\begin{aligned} E_z^{sca}(r, \phi) &= \sum_{n=-\infty}^{\infty} S_n H_n^{(1)}(k_0 r) \exp(jn\phi) \\ &= \sum_{n=-\infty}^{\infty} \sum_{m=0}^{\infty} S_n^{(m)} H_n^{(1)}(k_0 r) \exp(jn\phi) \end{aligned} \tag{34}$$

where (21), (25), and (29) give us the zeroth-, first-, and second-order contributions, respectively, as

$$S_n^{(0)} = E_1 S_{1,n}^{(0)} \tag{35a}$$

$$S_n^{(1)} = E_1 \sum_{m=-\infty}^{\infty} S_{1,n,m}^{(1)}(0) h_m \tag{35b}$$

$$S_n^{(2)} = E_1 \sum_{m=-\infty}^{\infty} \sum_{p=-\infty}^{\infty} S_{1,n,m,p}^{(2)}(0,0) h_m h_p \tag{35c}$$

and $S_{1,n}^{(0)}, S_{1,n,m}^{(1)}$, and $S_{1,n,m,p}^{(2)}$ can be calculated from (22), (26), and (30), respectively. The averaged scattering cross section is given by

$$\begin{aligned} \overline{\sigma}(\phi) &= \lim_{r \to \infty} 2\pi r \frac{\overline{|E_z^{(s)}(r, \phi)|^2}}{|E_1|^2} \\ &= \frac{4}{k_0} \sum_{n=-\infty}^{\infty} \sum_{m=-\infty}^{\infty} j^{m-n} \frac{\overline{(S_n S_m^*)}}{|E_1|^2} \exp(j(n-m)\phi) \end{aligned} \tag{36}$$

$\overline{S_n S_m^*}$ can be evaluated to the second-order using (35)

$$\begin{aligned} \frac{\overline{(S_n S_m^*)}}{|E_1|^2} = S_{1,n}^{(0)} S_{1,m}^{(0)*} &+ \sum_{p=-\infty}^{\infty} S_{1,n,p}^{(1)}(0) S_{1,m,p}^{(1)*}(0) \rho_p \\ &+ S_{1,n}^{(0)} \sum_{p=-\infty}^{\infty} S_{1,m,p,-p}^{(2)*}(0,0) \rho_p \\ &+ S_{1,m}^{(0)*} \sum_{p=-\infty}^{\infty} S_{1,n,p,-p}^{(2)}(0,0) \rho_p \end{aligned} \tag{37}$$

where $\rho_p = \frac{1}{2\pi} \int_{-\pi}^{\pi} R(\phi) \exp(-jp\phi)\, d\phi$. For numerical validation, (36) and (37) are used to compute $\overline{\sigma}(\phi)$ for a Gaussian correlated surface: $R(\phi) = h_0^2 \exp(-\phi^2/\phi_0^2)$, h_0 being the root-mean-square (rms) surface roughness and $l = a\phi_0$ being the correlation length, which is then compared with a Monte Carlo simulation wherein $\sigma(\phi)$ for each instance of $h(\phi)$ was computed using the MoM (see [22] for the case of an exponentially correlated azimuthal roughness). Each instance of the rough surface $h(\phi)$ was generated by following a procedure similar to the one outlined in [23] to obtain a Gaussian correlation between different points on the rough surface. It is essential to take sufficiently large number of instances for the Monte Carlo simulation to converge, and it was observed that convergence was achieved with approximately 100 instances.

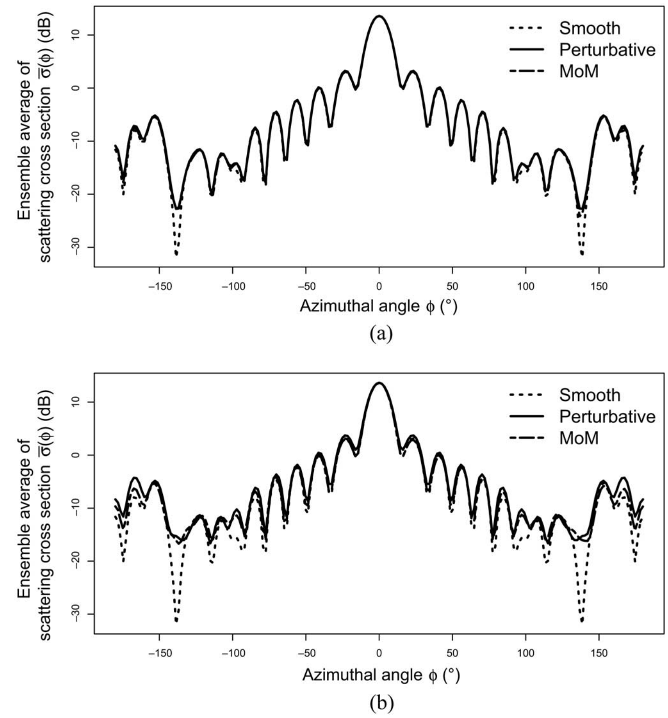

Fig. 2. Comparative plots of the ensemble average of the scattering cross section $\overline{\sigma}(\phi)$ as a function of ϕ for different h_0 calculated using the perturbative method, MoM, and the smooth cylinder approximation for the azimuthally rough cylinder. (a) $k_0 h_0 = 0.127$. (b) $k_0 h_0 = 0.314$. In all the calculations, $k_0 a = 12.566$, $k_0 l = 6.58$, permittivity $\epsilon_d = 2\epsilon_0$, and permeability $\mu_d = \mu_0$.

Finally, referring to Figs. 2(a) and 4(a), it can be seen that the perturbative method agrees with the MoM results for small values of rms roughness ($k_0 h_0 \sim 0.127$) and large correlation lengths ($k_0 l \sim 6.759$).

B. Cylinder With Axial Roughness

Consider now a case in which the cylinder roughness is only z dependant, and the cylinder is perfectly conducting. A PEC scatterer can either be analyzed by setting $\epsilon_d \to j\infty$ in the perturbative solution or by setting the internal fields to zero in the boundary conditions presented in Section II. Further, for an incident (and therefore scattered) field that depends only on r and z, it is straightforward to show from the Maxwell's equations that all the six field components can be expressed in terms of E_ϕ and H_ϕ. Here, we analyze only the TM polarization ($H_\phi = E_r = E_z = 0$), with a general azimuthally symmetric incident field given by

$$E_\phi^{inc} = \int_{-\infty}^{\infty} A^{inc}(k) H_1^{(2)}(\beta_0(k) r) \exp(jkz)\, dk \tag{38}$$

where $A^{inc}(k)$ is the "envelope" of the cylindrical waves constituting the incident field. The perturbative solution

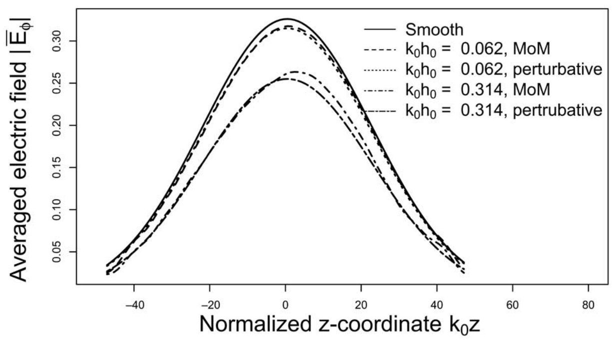

Fig. 3. Comparative plots of the ensemble average of the azimuthal electric field $|\overline{E}_\phi(r,z)|$ as a function of z for different h_0 calculated using the perturbative method, MoM, and the smooth cylinder approximation for a PEC cylinder with z-dependant roughness. In all the calculations, $k_0 a = 12.566$, $k_0 l = 12.566$, $k_0 w_0 = 31.42$, and $k_0 r = 15.71$.

presented in Section II can be specialized to the following expressions:

$$E_\phi^{sca} = \int_{-\infty}^{\infty} \sum_{n=0}^{\infty} A^{(n)}(k) H_1^{(1)}(\beta_0(k)r)\,dk \tag{39}$$

where

$$A^{(0)}(k) = \chi(k) A^{inc}(k) \tag{40a}$$

$$A^{(1)}(k) = \int_{-\infty}^{\infty} \zeta(k,k') A^{inc}(k-k') \tilde{h}_0(k')\,dk' \tag{40b}$$

$$A^{(2)}(k) = \int_{-\infty}^{\infty}\int_{-\infty}^{\infty} \Gamma(k,k',k'') A^{inc}(k-k'-k'') \tilde{h}_0(k')\tilde{h}_0(k'')\,dk'dk''. \tag{40c}$$

The coefficients $\chi(k), \zeta(k,k')$, and $\Gamma(k,k',k'')$ are given by

$$\chi(k) = -\frac{H_1^{(1)}(\beta_0(k)a)}{H_1^{(2)}(\beta_0(k)a)} \tag{41a}$$

$$\zeta(k,k') = -\frac{\beta_0(k-k')H_1^{(1)}(\beta_0(k-k')a)}{H_1^{(2)}(\beta_0(k)a)} \times \left[\frac{H_1^{(1)'}(\beta_0(k-k')a)}{H_1^{(1)}(\beta_0(k-k')a} - \frac{H_2^{(1)'}(\beta_0(k-k')a)}{H_2^{(1)}(\beta_0(k-k')a}\right] \tag{41b}$$

$$\Gamma(k,k',k'') = -\zeta(k-k'',k')\beta_0(k-k'')H_1^{(2)'}(\beta_0(k-k'')a) - \frac{\beta_0^2(k-k'-k'')}{2}\Big[H_1^{(1)''}(\beta_0(k-k'-k'')a) + \chi(k-k'-k'')H_1^{(2)''}(\beta_0(k-k'-k'')a)\Big]. \tag{41c}$$

If the autocorrelation function of the rough surface $R(z) = \overline{h(z+Z)h(Z)}$ is known, it is a simple matter to express the statistical properties of the scattered fields in terms of $R(z)$, for instance

$$\overline{E}_\phi(r,z) = \int_{-\infty}^{\infty} (A^{(0)}(k) + \overline{A^{(2)}(k)}) H_1^{(2)}(\beta_0(k)r)\exp(jkz)\,dk \tag{42}$$

where, from (40c)

$$\overline{A^{(2)}(k)} = A^{inc}(k)\int_{-\infty}^{\infty} \rho(k')\Gamma(k,k',-k')\,dk' \tag{43}$$

with $\rho(k) = \frac{1}{2\pi}\int_{-\infty}^{\infty} R(z)\exp(-jkz)\,dz$. For the purpose of comparison of the perturbative solution with MoM results, we choose to compute $\overline{E}_\phi(r,z)$ using the MoM for a Gaussian correlated surface: $R(z) = h_0^2\exp(-z^2/l^2)$, where h_0 is the rms roughness and l is the correlation length, and compare it with (42). Moreover, since the MoM simulation is possible only if the cylinder is *finite*, we assume a Gaussian incident beam, $A^{inc}(k) = \exp(-w_0^2k^2/4)$: w_0 being the waist size of the Gaussian beam, which is taken to be smaller than the length of the cylinder so as to reduce the edge diffraction effects [21], [23]. A Monte Carlo simulation was performed to compute the ensemble average of $\overline{E}_\phi(r,z)$, wherein each instance was analyzed using MoM, and 75 instances were required to achieve convergence in $\overline{E}_\phi(r,z)$. Observe from Figs. 4 and 5, similar to the case with azimuthal roughness, the MoM and the perturbative solutions agree for small rms roughness ($k_0h_0 \sim 0.062$) and large correlation lengths ($k_0 l \sim 12.56$).

IV. Results and Discussions

In the following sections, we investigate the validity of the perturbative solution derived in Section II-B. To demonstrate the validity of the solution, we compare our results with those obtained via the MoM. For the sake of convenience, we analyze the reduced cases of an azimuthally rough or axially rough cylinder introduced in Section III.

A. Validity of the Perturbative Solution

The validity of the perturbative solution presented in Section II depends on the correlation length l and the rms surface roughness h_0 of the scatterer in question. Figs. 2 and 3 show the comparison of the perturbative solution with the MoM simulation for different rms roughness values h_0. By an exhaustive comparison between the MoM and the perturbative method, it was found that the agreement between the perturbative and MoM simulation is acceptable within the range $k_0h_0 < 0.314$ for both azimuthal and z-dependant roughness, beyond which the perturbative solution deviates significantly from the MOM results.

The correlation length l governs the magnitude of the derivatives, $\partial h/\partial z$, or $\partial h/\partial\phi$. It is convenient to define the slope s corresponding to the rough surface via $s = h_0/l$.

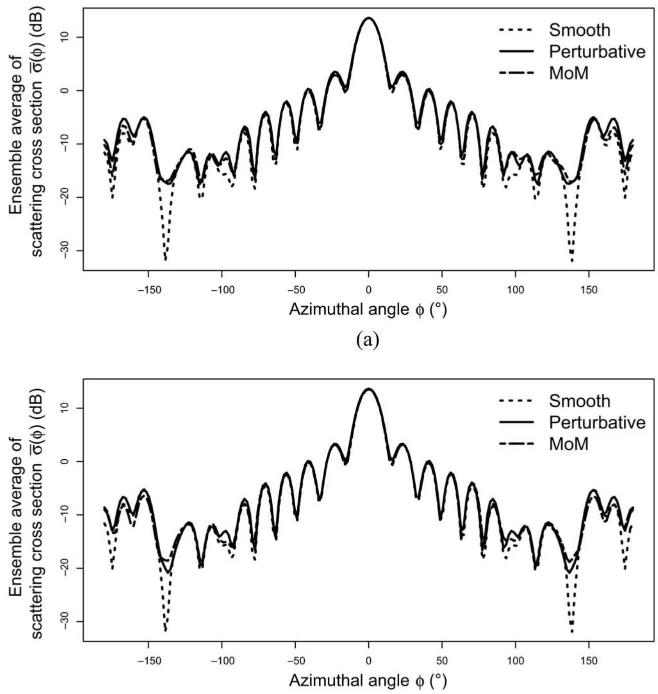

Fig. 4. Comparative plots of the ensemble average of the scattering cross section $\overline{\sigma}(\phi)$ as a function of ϕ for different correlation lengths l and slopes s calculated using the perturbative method, MoM, and the smooth cylinder approximation. (a) $k_0 l = 6.579$ and $s = 0.038$. (b) $k_0 l = 0.877$ and $s = 0.286$. In all the calculations, $k_0 a = 12.566$, $k_0 h_0 = 0.251$, $\epsilon_d = 2\epsilon_0$, and $\mu_d = \mu_0$.

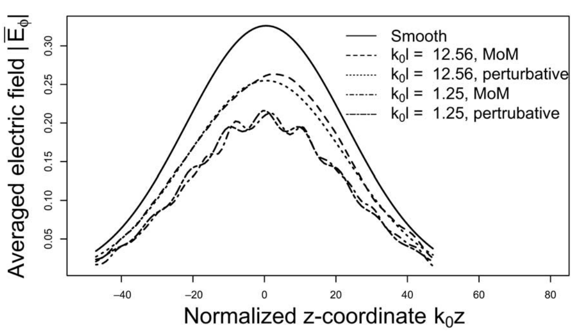

Fig. 5. Comparative plots of the ensemble average of the azimuthal electric field $|\overline{E}_\phi(r, z)|$ as a function of z for different l calculated using the perturbative method, MoM, and the smooth cylinder approximation for a PEC cylinder with z-dependant roughness. In all the calculations, $k_0 a = 12.566$, $k_0 h_0 = 0.314$, $k_0 w_0 = 31.42$, and $k_0 r = 15.71$.

The perturbative solution is expected to break down for large s or small l since an implicit assumption in the perturbative solution is that $h(\phi, z)$ and its derivatives are small. By comparing the perturbative solution with the MoM for different l (examples of which are shown in Figs. 4 and 5), it was found that the perturbative solution agrees with the MOM results for $s < 0.25$ for both azimuthal and z-dependant roughness.

B. Analysis of Rough Cylinders of Finite Height

As was stated earlier, the perturbative analysis presented in Section II yields not only the scattered fields, but also the fields inside the dielectric cylinder (17). Following the method presented by Hulst and Van De Hulst [17] and Seker and Schneider [18], the fields inside the finite cylinder are approximated by the fields inside the infinite cylinder. The scattered field can then be expressed in terms of the fields inside the cylinder. For instance, in a nonmagnetic medium, the scattered field $\mathbf{E}^{sca}$ can be computed from

$$\mathbf{E}^{sca}(\mathbf{r}) = \frac{k_0^2(\epsilon_d - \epsilon_0)}{4\pi\epsilon_0} \int_V \mathbf{E}^{cyl}(\mathbf{r}') \frac{e^{jk_0|\mathbf{r}-\mathbf{r}'|}}{|\mathbf{r}-\mathbf{r}'|} d^3\mathbf{r}' \qquad (44)$$

where $\mathbf{E}^{cyl}$ are the fields inside the cylinder and V is the volume of the finite cylinder. Note that the limits of the integral in (44) will depend on the rough surface and the integral can itself be evaluated perturbatively to any desired order in the roughness function.

C. General Considerations

The results obtained above, namely that a second-order perturbative solution for scattering from a rough cylinder is valid in the range of roughness h_0 and slope s given by $k_0 h_0 < 0.314$ and $s < 0.25$, are reminiscent of and similar to the results obtained for scattering from a randomly rough surface [6], [24]. Although the above-mentioned bounds are valid for the reduced cases (of an axially or azimuthally rough cylinder), we qualitatively expect these bounds to be a good approximation to the bounds for a full three-dimensional (3-D) case [with roughness of the form $h(\phi, z)$], provided that the surface roughness of the 3-D scatterer is described by a similar autocorrelation function. A quantitative validation for the full 3-D case is part of future work.

Additionally, observe that the zeroth-order scattered field (21) is entirely along $k_z = k_0 \cos\alpha$, i.e., it is scattered entirely in the specular direction. The first-order scattered field, on the other hand, has no specular component [since, from (25) $\overline{s_n^{(1)}(k)} = 0$]. However, the second-order scattered field (29) has a finite specular component. This can easily be seen by computing $\overline{s_n^{(2)}(k)}$ which results in

$$\overline{s_n^{(2)}(k)} = \left[\sum_{m=-\infty}^{\infty} \sum_{i=1}^{2} \int_{-\infty}^{\infty} S_{i,n,m,-m}^{(2)}(k_0\cos\alpha, k') E_i \right. \\ \left. \times\, \tilde{\rho}_m(k' - k_0\cos\alpha) dk' \right] \delta(k - k_0\cos\alpha) \quad (45)$$

where $\tilde{\rho}_n(k) = \frac{1}{4\pi^2} \int_0^{2\pi} \int_{-\infty}^{\infty} R(\phi, z) \exp(-j(n\phi + kz)) d\phi dz$ with $R(\phi, z) = \overline{h(\Phi, Z) h(\Phi + \phi, Z + z)}$ being the autocorrelation function of the roughness $h(\phi, z)$. The second-order results that have been derived in Section II can therefore be used to account for the impact of roughness of the cylinder in specularly scattered fields.

We emphasize that the scattered fields and the resulting scattering cross sections that have been previously derived are very simple to evaluate numerically. As was shown in Section III, an expression for the ensemble average of the scattering cross section can be derived in terms of the correlation function of the stochastic roughness. Evaluation of the average scattering cross section, and in general the electromagnetic fields, amounts to a simple numerical evaluation of this expression. Within the region of validity of the perturbative solution, this is computationally simpler and faster than the other numerical methods such as the MoM, where we would have to solve a large system of linear equations to calculate the scattered field for just a single instance of the rough cylinder. For instance, in the MoM analysis presented in Figs. 2 and 4, we needed to solve a 600 × 600 dense matrix system for each instance of the rough cylinder, and this process was repeated ∼100 times for obtaining a converged ensemble average of the scattering cross section.

The implications of these results to remote-sensing studies, particularly to scattering from trees or branches in the centimeter–millimeter wavelength range, are immediate. This is because the deviation from smooth-cylinder scattering becomes appreciable as the rms roughness of the surface increases and becomes comparable to the wavelength. This can also be seen in Fig. 2(a) and (b). Of course, this translates into additional data that need to be collected on a field work campaign, namely the measurement of trunk surface roughness, correlation length, and permittivity. However, since the computational overhead of incorporating roughness is minimal, the anticipated enhancement in science' returned from this exercise is worthwhile.

APPENDIX A
PERTURBATIVE SOLUTION

The scattering problem in Section II-B was formulated in terms of E_z and H_z. Knowing E_z and H_z, the remaining four field components can be calculated using the following equations:

$$\tilde{E}_r = \frac{j\eta_m k_m}{\beta_m^2 r}\frac{\partial \tilde{H}_z}{\partial \phi} + \frac{jk}{\beta_m^2}\frac{\partial \tilde{E}_z}{\partial r} \tag{46a}$$

$$\tilde{E}_\phi = -\frac{j\eta_m k_m}{\beta_m^2}\frac{\partial \tilde{H}_z}{\partial r} + \frac{jk}{\beta_m^2 r}\frac{\partial \tilde{E}_z}{\partial \phi} \tag{46b}$$

$$\tilde{H}_r = \frac{jk}{\beta_m^2}\frac{\partial \tilde{H}_z}{\partial r} - \frac{jk_m}{\eta_m \beta_m^2 r}\frac{\partial \tilde{E}_z}{\partial \phi} \tag{46c}$$

$$\tilde{H}_\phi = \frac{jk}{\beta_m^2 r}\frac{\partial \tilde{H}_z}{\partial \phi} + \frac{jk_m}{\beta_m^2 \eta_m}\frac{\partial \tilde{E}_z}{\partial r} \tag{46d}$$

where $\tilde{E}_p = \frac{1}{2\pi}\int_{-\infty}^{\infty} E_p \exp(-jkz)\ dz$ and $\tilde{H}_p = \frac{1}{2\pi}\int_{-\infty}^{\infty} H_p \exp(-jkz)\ dz$ for $p = r, \phi,$ and z. Using the expansions given by (15)–(17) along with the perturbation series expansion of the coefficients (18) immediately results in (21)–(23) for the zeroth-order perturbation coefficients. The zeroth-order perturbation coefficients along with (46) can be used to calculate the zeroth-order perturbations in $\Delta\mathbf{E}$ and $\Delta\mathbf{H}$. For instance, $\Delta E_z^{(0)}$ can be calculated as

$$\Delta E_z^{(0)} = \sum_{n=-\infty}^{\infty}\int_{-\infty}^{\infty}\Big[\Big\{s_n^{(0)}(k)H_n^{(1)}(\beta_0 r) - a_n^{(0)}(k)J_n(\beta_d r)\Big\} \exp(jkz)\,dk - j^n E_1\sin\alpha J_n(k_0 r\sin\alpha)\exp(jk_0 r\sin\alpha)\Big]$$
$$\times \exp(jn\phi) = \sum_{n=-\infty}^{\infty}\int_{-\infty}^{\infty}\Bigg[\sum_{i=1}^{2}\Big\{S_{i,n}^{(0)}E_i H_n^{(1)}(\beta_0 r) - A_{i,n}^{(0)}E_i J_n(\beta_d r)\Big\}\delta(k - k_0\cos\alpha)\exp(jkz)\,dk - j^n E_1\sin\alpha J_n(k_0 r\sin\alpha)\exp(jk_0 r\sin\alpha)\Bigg]\exp(jn\phi). \tag{47}$$

Since $\int_{-\infty}^{\infty} f(k)\delta(k-\kappa)\,dk = f(\kappa)$, (47) can be simplified to

$$\Delta E_z^{(0)} = \sum_{n=-\infty}^{\infty}\sum_{i=1}^{2} E_i Z_{i,n,E}^{(0)}(r)\exp(j(n\phi + k_0 z\cos\alpha)) \tag{48}$$

where (α_d is defined by $\cos\alpha_d = k_0/k_d\cos\alpha_0$)

$$Z_{1,n,E}^{(0)}(r) = S_{1,n}^{(0)}H_n^{(1)}(k_0 r\sin\alpha) - A_{1,n}^{(0)}J_n(k_d r\sin\alpha_d) + j^n\sin\alpha J_n(k_0 r\sin\alpha) \tag{49a}$$

$$Z_{2,n,E}^{(0)}(r) = S_{2,n}^{(0)}H_n^{(1)}(k_0 r\sin\alpha) - A_{2,n}^{(0)}J_n(k_d r\sin\alpha_d). \tag{49b}$$

Similar expressions can be derived for the zeroth-order perturbation in the other coefficients. Thus,

$$\Delta X_q^{(0)}(r) = \sum_{n=-\infty}^{\infty}\sum_{i=1}^{2} E_i Q_{i,n,X}^{(0)}(r)\exp(j(n\phi + k_0 z\cos\alpha))$$
$$\text{for } X \in \{E, H\}, q \in \{r, \phi, z\}, Q \in \{R, \Phi, Z\} \tag{50}$$

where

$$Z_{1,n,H}^{(0)}(r) = G_{1,n}^{(0)}H_n^{(1)}(k_0 r\sin\alpha) - B_{1,n}^{(0)}J_n(k_d r\sin\alpha_d) \tag{51a}$$

$$Z_{2,n,H}^{(0)}(r) = G_{2,n}^{(0)}H_n^{(1)}(k_0 r\sin\alpha) - B_{2,n}^{(0)}J_n(k_d r\sin\alpha_d) + \frac{1}{\eta_0}j^n\sin\alpha J_n(k_0 r\sin\alpha) \tag{51b}$$

$$\begin{aligned}\Phi_{1,n,E}^{(0)}(r) = &-\frac{j\eta_0}{\sin\alpha}G_{1,n}^{(0)}H_n^{(1)\prime}(k_0 r\sin\alpha) - \frac{n\cos\alpha}{k_0 r\sin^2\alpha}S_{1,n}^{(0)}H_n^{(1)}(k_0 r\sin\alpha) \\ &+ \frac{j\eta_0}{\sin\alpha_d}B_{1,n}^{(0)}J_n'(k_d r\sin\alpha_d) + \frac{n\cos\alpha_d}{k_d r\sin^2\alpha_d}A_{1,n}^{(0)}J_n(k_d r\sin\alpha_d) \\ &- \frac{nj^n\cot\alpha}{k_0 r}J_n(k_0 r\sin\alpha)\end{aligned} \tag{51c}$$

$$\begin{aligned}\Phi_{2,n,E}^{(0)}(r) = &-\frac{j\eta_0}{\sin\alpha}G_{2,n}^{(0)}H_n^{(1)\prime}(k_0 r\sin\alpha) - \frac{n\cos\alpha}{k_0 r\sin^2\alpha}S_{2,n}^{(0)}H_n^{(1)}(k_0 r\sin\alpha) \\ &+ \frac{j\eta_0}{\sin\alpha_d}B_{2,n}^{(0)}J_n'(k_d r\sin\alpha_d) + \frac{n\cos\alpha_d}{k_d r\sin^2\alpha_d}A_{2,n}^{(0)}J_n(k_d r\sin\alpha_d) \\ &- j^{n+1}J_n'(k_0 r\sin\alpha)\end{aligned} \tag{51d}$$

$$\begin{aligned}\Phi_{1,n,H}^{(0)}(r) = &-\frac{n\cos\alpha}{k_0 r\sin^2\alpha}G_{1,n}^{(0)}H_n^{(1)}(k_0 r\sin\alpha)\\ &+\frac{jS_{1,n}^{(0)}}{\eta_0\sin\alpha}H_n^{(1)'}(k_0 r\sin\alpha)\\ &+\frac{n\cos\alpha_d}{k_d r\sin^2\alpha_d}B_{1,n}^{(0)}J_n(k_d r\sin\alpha_d)\\ &+\frac{j}{\eta_d\sin\alpha_d}A_{1,n}^{(0)}J_n'(k_d r\sin\alpha_d)\\ &+\frac{j^{n+1}}{\eta_0}J_n'(k_0 r\sin\alpha)\end{aligned} \tag{51e}$$

$$\begin{aligned}\Phi_{2,n,H}^{(0)}(r) = &-\frac{n\cos\alpha}{k_0 r\sin^2\alpha}G_{2,n}^{(0)}H_n^{(1)}(k_0 r\sin\alpha)\\ &+\frac{jS_{2,n}^{(0)}}{\eta_0\sin\alpha}H_n^{(1)'}(k_0 r\sin\alpha)\\ &+\frac{n\cos\alpha_d}{k_d r\sin^2\alpha_d}B_{2,n}^{(0)}J_n(k_d r\sin\alpha_d)\\ &+\frac{j}{\eta_d\sin\alpha_d}A_{2,n}^{(0)}J_n'(k_d r\sin\alpha_d)\\ &-\frac{nj^n\cot\alpha}{\eta_0 k_0 r}J_n(k_0 r\sin\alpha)\end{aligned} \tag{51f}$$

$$\begin{aligned}R_{1,n,E}^{(0)}(r) = &-\frac{n\eta_0}{k_0 r\sin^2\alpha}G_{1,n}^{(0)}H_n^{(1)}(k_0 r\sin\alpha)\\ &+j\cot\alpha S_{1,n}^{(0)}H_n^{(1)'}(k_0 r\sin\alpha)\\ &+\frac{\eta_d nB_{1,n}^{(0)}}{k_d r\sin^2\alpha_d}J_n(k_d r\sin\alpha_d)\\ &-j\cot\alpha_d A_{1,n}^{(0)}J_n'(k_d r\sin\alpha_d)\\ &+j^{n+1}\cos\alpha J_n'(k_0 r\sin\alpha)\end{aligned} \tag{51g}$$

$$\begin{aligned}R_{2,n,E}^{(0)}(r) = &-\frac{n\eta_0}{k_0 r\sin^2\alpha}G_{2,n}^{(0)}H_n^{(1)}(k_0 r\sin\alpha)\\ &+j\cot\alpha S_{2,n}^{(0)}H_n^{(1)'}(k_0 r\sin\alpha)\\ &+\frac{\eta_d nB_{2,n}^{(0)}}{k_d r\sin^2\alpha_d}J_n(k_d r\sin\alpha_d)\\ &-j\cot\alpha_d A_{2,n}^{(0)}J_n'(k_d r\sin\alpha_d)\\ &-\frac{nj^n}{k_0 r\sin\alpha}J_n(k_0 r\sin\alpha)\end{aligned} \tag{51h}$$

$$\begin{aligned}R_{1,n,H}^{(0)}(r) = &\,j\cot\alpha G_{1,n}^{(0)}H_n^{(1)'}(k_0 r\sin\alpha)\\ &+\frac{nS_{1,n}^{(0)}}{\eta_0 k_0 r\sin^2\alpha}H_n^{(1)}(k_0 r\sin\alpha)\\ &-j\cot\alpha_d B_{1,n}^{(0)}J_n(k_d r\sin\alpha_d)\\ &-\frac{nA_{1,n}^{(0)}}{\eta_d k_d r\sin^2\alpha_d}J_n(k_d r\sin\alpha_d)\\ &+\frac{nj^n}{\eta_0 k_0 r\sin\alpha}J_n(k_0 r\sin\alpha)\end{aligned} \tag{51i}$$

$$\begin{aligned}R_{2,n,H}^{(0)}(r) = &\,j\cot\alpha G_{2,n}^{(0)}H_n^{(1)'}(k_0 r\sin\alpha)\\ &+\frac{nS_{2,n}^{(0)}}{\eta_0 k_0 r\sin^2\alpha}H_n^{(1)}(k_0 r\sin\alpha)\\ &-j\cot\alpha_d B_{2,n}^{(0)}J_n(k_d r\sin\alpha_d)\\ &-\frac{nA_{2,n}^{(0)}}{\eta_d k_d r\sin^2\alpha_d}J_n(k_d r\sin\alpha_d)\\ &+\frac{j^{n+1}\cot\alpha}{\eta_0}J_n'(k_0 r\sin\alpha).\end{aligned} \tag{51j}$$

To evaluate the first-order perturbation coefficients, we employ the boundary conditions given by (9). These boundary conditions can be translated into a set of linear equations in the first-order perturbation coefficients. For instance, consider (9a)

$$\Delta E_z^{(1)}\Big|_{r=a} = -h\frac{\partial\Delta E_z^{(0)}}{\partial r}\Big|_{r=a} - \frac{\partial h}{\partial z}\Delta E_r^{(0)}\Big|_{r=a}. \tag{52}$$

But

$$\Delta E_z^{(1)}\Big|_{r=a} = \sum_{n=-\infty}^{\infty}\int_{-\infty}^{\infty}\left[s_n^{(1)}(k)H_n^{(1)}(\beta_0 a) - a_n^{(1)}(k)J_n(\beta_d a)\right] \exp(jkz)\,dk\exp(jn\phi) \tag{53}$$

and from (52)

$$\begin{aligned}\Delta E_z^{(1)}\Big|_{r=a} = &-\left[\sum_{n=-\infty}^{\infty}\int_{-\infty}^{\infty}\tilde{h}_n(k)\exp(j(n\phi+kz))\,dk\right]\\ &\times\left[\sum_{m=-\infty}^{\infty}\sum_{i=1}^{2}E_i Z_{i,m,E}^{(0)'}(a)\exp(j(m\phi+k_0 z\cos\alpha))\right]\\ &-\left[\sum_{n=-\infty}^{\infty}\int_{-\infty}^{\infty}jk\tilde{h}_n(k)\exp(j(n\phi+kz))\,dk\right]\\ &\times\left[\sum_{m=-\infty}^{\infty}\sum_{i=1}^{2}E_i R_{i,m,E}^{(0)}(a)\exp(j(m\phi+k_0 z\cos\alpha))\right].\end{aligned} \tag{54}$$

Comparing the coefficients of $\exp(j(kz+n\phi))$ between (53) and (54)

$$\begin{aligned}&s_n^{(1)}(k)H_n^{(1)}(\beta_0 a) - a_n^{(1)}(k)J_n(\beta_d a)\\ &\quad=\sum_{m=-\infty}^{\infty}\sum_{i=1}^{2}\Big[E_i\Big(-Z_{i,n-m,E}^{(0)'}(a)j(k-k_0\cos\alpha)\\ &\quad\times R_{i,n-m,E}^{(0)'}(a)\Big)\Big]\tilde{h}_m(k-k_0\cos\alpha).\end{aligned} \tag{55}$$

A similar manipulation of the other first-order boundary conditions results in (25) and (26) for the first-order coefficients. These can, in turn, be used for evaluating the first-order perturbation in $\mathbf{\Delta E}$ and $\mathbf{\Delta H}$ which are needed for the calculation of the second-order coefficients. Consider, for instance, $\Delta E_z^{(1)}$

$$\Delta E_z^{(1)} = \sum_{n=-\infty}^{\infty} \int_{-\infty}^{\infty} \left(s_n^{(1)}(k) H_n^{(1)}(\beta_0 r) - a_n^{(1)}(k) J_n(\beta_d r) \right) \exp(jkz)\, dk \exp(jn\phi)$$
$$= \sum_{n=-\infty}^{\infty} \sum_{m=-\infty}^{\infty} \sum_{i=1}^{2} \int_{-\infty}^{\infty} \left(S_{i,n,m}^{(1)}(k) H_n^{(1)}(\beta_0 r) - A_{i,n,m}^{(1)}(k) J_n(\beta_d r) \right) E_i h_m(k - k_0 \cos\alpha) \exp(j(kz + n\phi)) dk \quad (56)$$

or equivalently

$$\Delta E_z^{(1)}(r) = \sum_{n=-\infty}^{\infty} \sum_{m=-\infty}^{\infty} \sum_{i=1}^{2} \int_{-\infty}^{\infty} E_i Z_{i,n,m,E}^{(1)}(r,k) \tilde{h}_m(k - k_0 \cos\alpha) \exp(j(n\phi + kz))\, dk \quad (57)$$

where

$$Z_{i,n,m,E}^{(1)}(r,k) = S_{i,n,m}^{(1)}(k) H_n^{(1)}(\beta_0 r) - A_{i,n,m}^{(1)}(k) J_n(\beta_d r). \quad (58)$$

Similar expressions can be derived for the first-order perturbation in the other components of $\mathbf{\Delta E}$ and $\mathbf{\Delta H}$

$$\Delta X_q^{(1)}(r) = \sum_{n=-\infty}^{\infty} \sum_{m=-\infty}^{\infty} \int_{-\infty}^{\infty} \sum_{i=1}^{2} E_i Q_{i,n,m,X}^{(1)}(r,k) \tilde{h}_m(k - k_0 \cos\alpha) \exp(j(n\phi + kz))\, dk \quad (59)$$

where

$$Z_{i,n,m,H}^{(1)}(r,k) = G_{i,n,m}^{(1)}(k) H_n^{(1)}(\beta_0 r) - B_{i,n,m}^{(1)}(k) J_n(\beta_d r) \quad (60a)$$

$$\Phi_{i,n,m,E}^{(1)}(r,k) = -\frac{j\eta_0 k_0}{\beta_0} G_{i,n,m}^{(1)} H_n^{(1)'}(\beta_0 r) - \frac{nk}{\beta_0^2 r} S_{i,n,m}^{(1)} H_n^{(1)}(\beta_0 r) + \frac{j\eta_d k_d}{\beta_d} B_{i,n,m}^{(1)} J_n'(\beta_d r) + \frac{nk}{\beta_d^2 r} A_{i,n,m}^{(1)} J_n(\beta_d r) \quad (60b)$$

$$\Phi_{i,n,m,H}^{(1)}(r,k) = -\frac{nk}{\beta_0^2 r} G_{i,n,m}^{(1)} H_n^{(1)}(\beta_0 r) + \frac{jk_0}{\eta_0 \beta_0} S_{i,n,m}^{(1)} H_n^{(1)'}(\beta_0 r) + \frac{nk}{\beta_d^2 r} B_{i,n,m}^{(1)} J_n(\beta_d r) - \frac{jk_d}{\eta_d \beta_d} A_{i,n,m}^{(1)} J_n'(\beta_d r) \quad (60c)$$

$$R_{i,n,m,E}^{(1)}(r,k) = -\frac{n\eta_0 k_0}{\beta_0^2 r} G_{i,n,m}^{(1)} H_n^{(1)}(\beta_0 r) + \frac{jk}{\beta_0} S_{i,n,m}^{(1)} H_n^{(1)'}(\beta_0 r) + \frac{n\eta_d k_d}{\beta_d^2 r} B_{i,n,m}^{(1)} J_n(\beta_d r) - \frac{jk}{\beta_d} A_{i,n,m}^{(1)} J_n'(\beta_d r) \quad (60d)$$

$$R_{i,n,m,H}^{(1)}(r,k) = \frac{jk}{\beta_0} G_{i,n,m}^{(1)} H_n^{(1)'}(\beta_0 r) + \frac{nk_0}{\eta_0 \beta_0^2 r} S_{i,n,m}^{(1)} H_n^{(1)}(\beta_0 r) - \frac{jk}{\beta_d} B_{i,n,m}^{(1)} J_n'(\beta_d r) - \frac{nk_d}{\eta_d \beta_d^2 r} A_{i,n,m}^{(1)} J_n(\beta_d r). \quad (60e)$$

Evaluation of the second-order perturbation coefficients requires the imposition of the boundary conditions given by (10). Consider, for instance, (10a)

$$\Delta E_z^{(2)}\Big|_{r=a} = -h \frac{\partial \Delta E_z^{(1)}}{\partial r}\Bigg|_{r=a} - \frac{h^2}{2} \frac{\partial^2 \Delta E_z^{(0)}}{\partial r^2}\Bigg|_{r=a} - \frac{\partial h}{\partial z} \Delta E_r^{(1)}\Bigg|_{r=a} - h \frac{\partial h}{\partial z} \frac{\partial \Delta E_r^{(0)}}{\partial r}\Bigg|_{r=a}. \quad (61)$$

Since

$$\Delta E_z^{(2)}\Bigg|_{r=a} = \sum_{n=-\infty}^{\infty} \int_{-\infty}^{\infty} (s_n^{(2)}(k) H_n^{(1)}(\beta_0 a) - a_n^{(2)}(\beta_d a)) \exp(jn\phi) \exp(jkz)\, dk. \quad (62)$$

Also, using (61)

$$\Delta E_z^{(2)}|_{r=a} = -\left[\sum_{m=-\infty}^{\infty} \int_{-\infty}^{\infty} \tilde{h}_m(k) \exp(j(m\phi + kz))\, dk \right] \times \left[\sum_{n=-\infty}^{\infty} \sum_{m=-\infty}^{\infty} \sum_{i=1}^{2} \int_{-\infty}^{\infty} E_i Z_{i,n,m,E}^{(1)'}(a,k) \tilde{h}_m(k - k_0 \cos\alpha) \exp(j(n\phi + kz))\, dk \right]$$
$$- \frac{1}{2} \left[\sum_{m=-\infty}^{\infty} \int_{-\infty}^{\infty} \tilde{h}_m(k) \exp(jm\phi) \exp(jkz)\, dk \right]^2 \times \left[\sum_{n=-\infty}^{\infty} \sum_{i=1}^{2} E_i Z_{i,n,E}^{(0)''}(a) \exp(jn\phi) \exp(jk_0 r \cos\alpha) \right]$$
$$- \left[\sum_{m=-\infty}^{\infty} \int_{-\infty}^{\infty} jk\tilde{h}_m(k) \exp(jm\phi) \exp(jkz)\, dk \right] \times \left[\sum_{n=-\infty}^{\infty} \sum_{m=-\infty}^{\infty} \sum_{i=1}^{2} \int_{-\infty}^{\infty} E_i R_{i,n,m,E}^{(1)}(a,k) \tilde{h}_m(k - k_0 \cos\alpha) \exp(jkz)\, dk \exp(jn\phi) \right]$$
$$- \left[\sum_{m=-\infty}^{\infty} \int_{-\infty}^{\infty} jk\tilde{h}_m(k) \exp(j(m\phi + kz)) dk \right]$$

$$\times \left[\sum_{n=-\infty}^{\infty} \int_{-\infty}^{\infty} \tilde{h}_n(k) \exp(j(kz + n\phi)) dk \right]$$
$$\times \left[\sum_{n=-\infty}^{\infty} \sum_{i=1}^{2} E_i R_{i,n,E}^{(0)'}(a) \exp(jn\phi) \exp(jk_0 r \cos\alpha) \right]. \tag{63}$$

Comparing coefficients of $\exp(jkz)\exp(jn\phi)$ between (62) and (63)

$$s_n^{(2)}(k) H_n^{(1)}(\beta_0 a) - a_n^{(2)}(\beta_d a) = \sum_{m=-\infty}^{\infty} \sum_{p=-\infty}^{\infty}$$
$$\sum_{i=1}^{2} \int_{-\infty}^{\infty} E_i \left(-Z_{i,n-p,m,E}^{(1)'}(a,k') - \frac{Z_{i,n-p-m,E}^{(0)''}(a)}{2} \right.$$
$$\left. -j(k-k')(R_{i,n-p,m,E}^{(1)}(a,k') + R_{i,n-p-m,E}^{(0)'}(a)) \right)$$
$$\tilde{h}_m\left(k' - k_0 \cos\alpha\right) h_p\left(k - k'\right)\, dk'. \tag{64}$$

A similar manipulation of the other second-order boundary conditions results in (29) and (30). Higher order perturbation coefficients can also be evaluated by following a similar procedure.

References

[1] M. Karam and A. Fung, “Electromagnetic scattering from a layer of finite length, randomly oriented, dielectric, circular cylinders over a rough interface with application to vegetation,” *Remote Sens.*, vol. 9, no. 6, pp. 1109–1134, 1988.

[2] T. Chiu and K. Sarabandi, “Electromagnetic scattering interaction between a dielectric cylinder and a slightly rough surface,” *IEEE Trans. Antennas Propag.*, vol. 47, no. 5, pp. 902–913, May 1999.

[3] Y. C. Lin and K. Sarabandi, “Electromagnetic scattering model for a tree trunk above a tilted ground plane,” *IEEE Trans. Geosci. Remote Sens.*, vol. 33, no. 4, pp. 1063–1070, Jul. 1995.

[4] K. Sarabandi and F. T. Ulaby, “High frequency scattering from corrugated stratified cylinders,” *IEEE Trans. Antennas Propag.*, vol. 39, no. 4, pp. 512–520, Apr. 1991.

[5] A. E. El-Rouby, F. T. Ulaby, and A. Y. Nashashibi, “MMW scattering by rough lossy dielectric cylinders and tree trunks,” *IEEE Trans. Geosci. Remote Sens.*, vol. 40, no. 4, pp. 871–879, Apr. 2002.

[6] S. O. Rice, “Reflection of electromagnetic waves from slightly rough surfaces,” *Commun. Pure Appl. Math.*, vol. 4, nos. 2–3, pp. 351–378, 1951.

[7] P. Beckmann and A. Spizzichino, *The Scattering of Electromagnetic Waves From Rough Surfaces*, vol. 1. Norwood, MA, USA: Artech House, 1987, p. 511.

[8] J. T. Johnson, “Third-order small-perturbation method for scattering from dielectric rough surfaces,” *J. Opt. Soc. Amer. A*, vol. 16, no. 11, pp. 2720–2736, 1999.

[9] I. M. Fuks, “Wave diffraction by a rough boundary of an arbitrary plane-layered medium,” *IEEE Trans. Antennas Propag.*, vol. 49, no. 4, pp. 630–639, Apr. 2001.

[10] P. Imperatore, A. Iodice, and D. Riccio, *Boundary Perturbation Theory for Scattering in Layered Rough Structures*. Croatia: InTech, 2010.

[11] P. Imperatore, A. Iodice, and D. Riccio, “Volumetric-perturbative reciprocal formulation for scattering from rough multilayers,” *IEEE Trans. Antennas Propag.*, vol. 59, no. 3, pp. 877–887, Mar. 2011.

[12] H. Cabayan and R. Murphy, “Scattering of electromagnetic waves by rough perfectly conducting circular cylinders,” *IEEE Trans. Antennas Propag.*, vol. 21, no. 6, pp. 893–895, Nov. 1973.

[13] C. Eftimiu, “Electromagnetic scattering by rough conduction circular cylinders. I. Angular corrugation,” *IEEE Trans. Antennas Propag.*, vol. 36, no. 5, pp. 651–658, May 1988.

[14] C. Eftimiu, “Electromagnetic scattering by rough conducting circular cylinders,” *Radio Sci.*, vol. 23, no. 5, pp. 760–768, 1988.

[15] T. Tong, “Scattering by a slightly rough cylinder and a cylinder with an impedance boundary condition,” *Int. J. Electron. Theor. Exp.*, vol. 36, no. 6, pp. 767–772, 1974.

[16] E. Bahar and M. A. Fitzwater, “Scattering and depolarization by conducting cylinders with rough surfaces,” *Appl. Opt.*, vol. 25, no. 11, pp. 1826–1832, 1986.

[17] H. C. Hulst and H. Van De Hulst, *Light Scattering by Small Particles*. New York, NY, USA: Dover, 1957.

[18] S. Seker and A. Schneider, “Electromagnetic scattering from a dielectric cylinder of finite length,” *IEEE Trans. Antennas Propag.*, vol. 36, no. 2, pp. 303–307, Feb. 1988.

[19] W. C. Chew, *Waves and Fields in Inhomogeneous Media*, vol. 522. Piscataway, NJ, USA: IEEE Press, 1995.

[20] J. R. Wait, “Scattering of a plane wave from a circular dielectric cylinder at oblique incidence,” *Can. J. Phys.*, vol. 33, no. 5, pp. 189–195, 1955.

[21] R. Trivedi and U. K. Khankhoje, “Method of moments for computing electromagnetic scattering from a rough cylinder,” arXiv preprint, arXiv: 1505.03744 (math-NA), 2015 [Online]. Available: http://arxiv.org/abs/1505.03744

[22] R. Trivedi and U. K. Khankhoje, “A perturbative solution to plane wave scattering from a rough dielectric cylinder,” in *Proc. Prog. Electromagn. Res. Symp. (PIERS)*, pp. 1254–1258, 2015.

[23] E. I. Thorsos, “The validity of the Kirchhoff approximation for rough surface scattering using a Gaussian roughness spectrum,” *J. Acoust. Soc. Amer.*, vol. 83, no. 1, pp. 78–92, 1988.

[24] X. Gu, L. Tsang, H. Braunisch, and P. Xu, “Modeling absorption of rough interface between dielectric and conductive medium,” *Microw. Opt. Technol. Lett.*, vol. 49, no. 1, pp. 7–13, 2007.

Rahul Trivedi photograph and biography not available at the time of publication.

Uday K. Khankhoje photograph and biography not available at the time of publication.